A new marine geoid model for Argentina combining altimetry, shipborne gravity data and CHAMP/GRACE-type EGMs

C. Tocho✉
Facultad de Ciencias Astronómicas y Geofísicas, Paseo del Bosque s/n, 1900 La Plata, Argentina.
e-mail: ctocho@fcaglp.unlp.edu.ar

G.S. Vergos
Department of Geodesy and Surveying, Aristotle University of Thessaloniki, Univ. Box. 440, 54124, Thessaloniki, Greece.

M.G. Sideris
Department of Geomatics Engineering, University of Calgary, 2500 University Drive N.W., Calgary, Alberta, T2N 1N4, Canada.

Abstract: Marine geoid modeling in the Atlantic coastal region of Argentina is problematic. Firstly, because of the insufficient amount of available shipborne gravity data, which renders a purely gravimetric solution not feasible. Secondly, because of the very strong ocean currents, which affect the quality of satellite altimetry data, so that a purely altimetric model is too noisy even after low-pass filtering the Sea Surface Heights (SSHs) to remove (part of) the influence of the oceanographic signals. Thus, the recommended solution is to employ a combination method and use all the available gravity and altimetry data together. This is a suitable solution since (i) combination methods such as least-squares collocation and Input Output System Theory (IOST) inherently low-pass filter and weigh the data, and (ii) will make use of the altimetric heights to fill the gaps of the shipborne gravity data. Following this idea, purely altimetric, gravimetric and combined (using the IOST method) marine geoid models have been estimated for Argentina employing all available shipborne gravity data, satellite altimetry SSHs and the latest Earth Gravity Models (EGMs) developed from the missions of CHAMP and GRACE. The new EGMs are especially useful to assess the quality of the new geoids, especially against EGM96, which was used in an older ERS1-only solution for the same area. From the comparison of the estimated geoid models with respect to stacked TOPEX/Poseidon SSHs, we found that the altimetric model provides the best agreement while the combined one improves the accuracy (1σ) of the gravimetric solution.

Keywords. marine geoid, altimetry, shipborne gravity, IOST, "combined" EGM, GRACE, CHAMP

---

1 Introduction

Continuing with our prior investigation (Tocho et al., 2005), carried out in order to determine a high-accuracy and high-resolution geoid model for the Atlantic coastal region of Argentina, our study is focussed now on the improvement of our previous results using a "combined" EGM derived from the latest CHAMP and GRACE type of EGMs (Vergos et al.,

2004). It should be mentioned that this so-called "combined" EGM is not a new model determined from raw CHAMP (CHAllenging Minisatellite Payload) and GRACE (Gravity Recovery and Climate Experiment) data, but a combination of the harmonic coefficients of the latest EGMs from GFZ (GeoForschungsZentrum Potsdam) and Center of Space Research (CSR), University of Texas. Therefore, by inspecting the CHAMP and GRACE degree and error-degree variances, we defined which one was more accurate for different harmonic degrees, and then a "combined" EGM was developed, using the CHAMP EGM for n=2-7, the GRACE EGM for n=8-120 and EGM96 for n=121-360 (Vergos et al., 2004).

In the present study, pure gravimetric and altimetric geoid models as well as a combined solution using the Multiple Input Multiple Output System Theory (MIMOST) method (Sideris, 1996; Andritsanos and Tziavos, 2002; Vergos et al., 2005a) have been estimated.

The pure gravimetric and altimetric geoid models are single data source ones, i.e., they are computed from shipborne gravity and satellite altimetry data alone, respectively. A combined solution on the other hand, makes use of both data types. The latter solution was computed to investigate if the combined used of satellite altimetry and shipborne data will improve the estimated geoid model compared to the purely gravimetric one.

The area under study is in the eastern part of Argentina bounded between $-34^{\circ} \leq \varphi \leq -55^{\circ}$ and $290^{\circ} \leq \lambda \leq 304^{\circ}$, which is mainly a marine area including Falkland Islands.

The marine gravity data available were gravity anomalies provided by the Bureau Gravimétrique International (BGI, 2001). Since there were some gaps between the ship tracks, the KMS01 and the newest release KMS02, $2' \times 2'$ altimetry derived free-air gravity anomaly field (Andersen and Knudsen, 1998) have been used as fill in information. KMS02 is the newest compilation of a global altimetry-derived marine free-air gravity field by the KMS group at the National Danish Survey and Cadastre (Andersen and Knudsen, 2005).

The topographic/bathymetric data for the residual terrain model (RTM) reduction (Forsberg, 1984) were those of the Smith and Sandwell model (Smith and Sandwell, 1997), which resulted as a combination of depths derived from altimetry and echo soundings.

The necessary, to derive geoid heights from altimetric measurements, information about the quasi-stationary sea surface topography (QSST) was computed from the Dynamic Ocean Topography (DOT) model, EGM96 DOT model, which is a spherical harmonic expansion of the SST, complete to degree and order 20 (Lemoine et al., 1998). That model was derived during the simultaneous adjustment for the development of the EGM96 geopotential model.

Finally, the altimetric data consist of sea surface heights (SSHs) from the Geodetic Mission ERS1 GM and repeated TOPEX/POSEIDON (T/P) SSHs from the entire 3rd year of the satellite's mission (AVISO, 1998).

2 Geoid modeling

2.1 Altimetric geoid with ERS1 data

An altimetric satellite measures the time taken by a radar pulse to travel from the satellite to the sea surface and then back to the satellite receiver. Combined with precise satellite location data, altimetry measurements yield Sea Surface Heights (SSHs), i.e., the height of the sea above a reference ellipsoid of revolution. The derived SSHs have to be corrected for several geophysical effects (tides, tidal loading, ionosphere, wet and dry troposphere, inverse barometer and electromagnetic bias) and instrumental errors (ultra-stable oscillator, centre of gravity, corrections for instrument and algorithm effects that can not be modeled and waveforms). After applying the above corrections, Corrected Sea Surface Heights (CorSSHs) are available for the Geodetic Mission of ERS1.

The altimetric geoid was computed using 70510 CorSSHs from the ERS1 Geodetic Mission, which were constructed by applying all instrumental and geophysical corrections to the raw SSHs provided by AVISO (1998). The magnitude of these corrections was computed

from the available algorithms and models provided by AVISO itself. Table 1 presents the statistics of the 70510 corrected ERS1-GM SSHs for the area under study.

Sea Surface Heights contain information about both the geoid and the sea surface topography (SST); while the latter consists of a time-dependent and a nearly time-independent component (quasi-stationary part). Stacking the repeat tracks can eliminate the effect of the time-dependent component and part of the sea surface variability effects that influence the data. The corrected sea surface heights were then reduced from the MSS to the geoid for the QSST signal, which is the quasi-stationary part of the Sea Surface Topography. This was performed by estimating the QSST at each sub-satellite point (QSST in CorSSHs) and removing the contribution of the QSST from the corrected sea surface height value (CorSSHs-QSST). The quasi-stationary component of the SST is modeled by a spherical harmonic series of the Dynamic Ocean Topography (DOT) EGM96.DOT model (see Table 1). Table 1 also shows the statistics of the QSST in the area under study as well as the CorSSHs after removing the QSST.

The altimetric geoid model was then computed using a remove-compute-restore procedure, i.e., by first removing the contribution of the new combined geopotential model (N^{GMcomb}) from the corrected sea surface heights and then RTM-reducing to take into account the effect of the bathymetric masses to the geoid signal (N^{RTM}). The statistics of the geoid referenced to the new "combined" EGM (CorSSHs-QSST-N^{GMcomb}) as well as those of the residual geoid heights after the residual terrain model (RTM) reduction (CorSSHs-QSST-N^{GMcomb}- N^{RTM}) are tabulated in Table 1. The residual geoid heights in Table 1 indicate that some values may still contain some blunders and/or systematic errors so a simple three root mean square (3 rms) test was performed for blunder detection and a total of 438 points were removed.

The residual Sea Surface Heights after the 3 rms test (Nres) represent the medium wavelengths of the geoid heights and can be used to compute the subsequent altimetric geoid

solution. Point residual geoid heights (Nres) were gridded with a weighted means method with prediction power two on a grid of 3' by 3 .The gridding of the random distributed data was based on a weighted means method using the inverse of the square of the distance as the weight for each irregular observation. It was done using the program *geogrid* from GRAVSOFT software (Tscherning et al., 1992). The statistics of the gridded ERS1 residual geoid heights with no filter applied (Nres (no filtering)) are given in Table 1.

Due to the very high Sea Surface Variability (SSV) present in the residual field, the data were low-pass filtered with a Wiener type of filter empirically testing different cut-off frequencies ω_c. The selection of the cut-off frequency to be used was based on a maximum noise reduction with the minimum signal loss principle. Finally a cut-off frequency corresponding to (ω_c=22 km) was selected for the low-pass filtering procedures using a collocation type of filter assuming Kaula's rule for the geoid spectrum. The final altimetric geoid solution (Nalt) was obtained restoring the geopotential model (N^{GMcomb}) and the contribution of the bathymetry (N^{RTM}).

Table 1. Statistics of the ERS1-GM altimetric geoid processing. Unit: [m]

Remove step	*min*	*max*	*mean*	σ
70510 ERS1-GM CorSSHs	0.589	19.010	11.259	±3.079
QSST in CorSSHs	-0.692	0.083	-0.169	±0.128
CorSSHs-QSST	0.772	19.646	11.428	±3.081
N^{GMcomb}	1.112	18.889	11.075	±2.907
CorSSHs-QSST-N^{GMcomb}	-1.337	2.922	0.352	±0.338
N^{RTM}	-0.557	0.847	0.070	±0.158
CorSSHs-QSST-N^{GMcomb}- N^{RTM}	-1.361	2.892	0.282	±0.336
3 rms test for blunders detection ⇒ 438 points were removed				
Nres= CorSSHs-DOT-N^{GMcomb}- N^{RTM}	-1.266	1.316	0.273	±0.314
Gridding				
Nres (no filtering)	-1.036	1.285	0.276	±0.274
Area with very high SSV, The gridded Nres was low-pass filter with a cut-off frequency of 22 km				
Nres (ω_c=22 km)	-1.118	0.838	0.068	±0.253
Restore step	min	max	mean	σ
N^{GMcomb}	1.102	19.166	11.231	±2.874
N^{RTM}	-0.567	0.847	0.070	±0.153
Nalt	**0.794**	**19.384**	**11.368**	**±3.018**

2.2 Gravimetric geoid solution

The gravimetric geoid modeling was computed using 12823 shipborne free-air gravity anomalies provided by the Bureau Gravimétrique International (BGI). These data refer to the Geodetic Reference System 1967 (GRS67), thus as a pre-processing step, they were transformed to the Geodetic Reference System 1980 (GRS80) in order to be compatible with the altimetric data (Li and Sideris, 1997). Another pre-processing step needed was due to the fact that the gravity anomalies available were not free-air reduced. Therefore, a free-air was applied using the QSST values from the EGM96 DOT. 16961 altimetry-derived from the KMS01 and KMS02 global datasets were used to fill in the sparse coverage of shipborne gravity measurements offshore Argentina. The evaluation of these two global models in the area under study will be presented in the next section. In Figure 1, the distribution of the gravity data is depicted for visualization purposes.

The computation of the gravimetric geoid model was based on the classical remove-compute-restore technique. First, the contribution of the new "combined EGM" was removed and then the bathymetry was taken into account using an RTM reduction. The difference with the altimetric geoid determination is in fact that after the residual gravity anomalies were gridded the contribution of the bathymetry was restored prior the geoid height prediction (Dahl and Forsberg, 1998). The computation of the residual gravimetric geoid heights was carried out by applying the two-dimensional FFT approximate Stokes convolution on the 3 arc-minute by 3 arc-minute grid (Strang Van Hess, 1990) using program *fftgeoid* (Li, 1993).

$$N_{res} = \frac{R\Delta\varphi\Delta\lambda}{4\pi\gamma} F_I^{-1}\{\{F\{\Delta g \cos\varphi\}F(\Delta\varphi, \Delta\lambda, \varphi_m)\}\} \quad (1)$$

where N_{res} are the estimated residual gravimetric geoid heights and F, F^{-1} denote the direct and inverse 2D Fourier transforms. The final gravimetric geoid solutions were computed by restoring the contribution of the geopotential model.

The statistics of the gravimetric geoid processing using the KMS01 and KMS02 datasets are presented in Tables 2 and 3, respectively.

Table 2. Statistics of gravimetric geoid model processing with KMS01 data.

Remove step Unit:[mGal]	*min*	*max*	*mean*	σ
Δg_{FA}	-133.0	142.57	3.49	±22.71
Δg^{GMcomb}	-112.91	114.16	1.92	±21.37
Δg_{FA} - Δg^{GMcomb}]	-80.61	63.21	1.57	±9.46
Δg^{RTM}	-34.11	32.98	0.28	±3.58
$\Delta g_{red} = \Delta g_{FA}$ - Δg^{GMcomb} - Δg^{RTM}	-54.98	61.78	1.29	±9.32
3 rms test for blunders detection ⇒ 653 points were removed				
$\Delta g_{red} = \Delta g_{FA}$ - Δg^{GMcomb} - Δg^{RTM}	-28.23	28.20	1.42	±7.65
Δg_{red} ⇒Gridding 3 arc-minute by 3 arc-minute				
Δg_{red} grid	-27.92	27.62	0.99	±7.11
Δg^{RTM}	-34.30	35.88	0.53	±4.35
Δg_{res} grid = Δg_{red} grid + Δg^{RTM} grid	-35.20	46.68	1.51	±7.40
Residual geoid heights computed ⇒2D FFT spherical Stokes kernel convolution (Strang Van Hess, 1990) computed with integration radius ~10 km				
Nres [m]	-0.445	0.408	0.013	±0.076
Restore step Unit:[m]	*min*	*max*	*mean*	σ
N^{GMcomb}	1.102	19.166	11.231	±2.873
Ngrav	**1.079**	**19.079**	**11.249**	**±2.869**

Table 3. Statistics of gravimetric geoid model processing with KMS02 data.

Remove step Unit:[mGal]	*min*	*max*	*mean*	σ
Δg_{FA}	-133.03	142.57	3.70	±22.74
Δg^{GMcomb}	-112.91	114.16	1.92	±21.37
Δg_{FA} – Δg^{GMcomb}]	-80.61	63.21	1.78	±9.59
Δg^{RTM}	-34.11	32.98	0.28	±3.58
$\Delta g_{red} = \Delta g_{FA}$ - Δg^{GMcomb} – Δg^{RTM}	-54.98	61.78	1.50	±9.44
3 rms test for blunders detection ⇒ 575 points were removed				
$\Delta g_{red} = \Delta g_{FA}$ - Δg^{GMcomb} – Δg^{RTM}	-29.78	29.76	1.60	±7.93
Δg_{red} ⇒Gridding 3 arc-minute by 3 arc-minute				
$\Delta g_{red\ grid}$	-29.27	28.99	1.03	±7.31
Δg^{RTM}	-34.30	35.88	0.53	±4.30
Δg_{res} grid = Δg_{red} grid + Δg^{RTM} grid	-46.68	49.59	1.56	±7.56
Residual geoid heights computed ⇒2D FFT spherical Stokes kernel convolution (Strang Van Hess, 1990) computed with integration radius ~10 km				
Nres [m]	-0.445	0.406	0.014	±0.078
Restore step Unit:[m]	*min*	*max*	*mean*	σ
N^{GMcomb} [m]	1.102	19.166	11.231	±2.873
Ngrav	**1.079**	**19.096**	**11.245**	**±2.869**

2.2.1 Validation of KMS01 and KMS02 altimetry-derived free-air gravity anomalies

KMS01 and KMS02 altimeter-derived gravity anomaly grids offshore Argentina were compared with one another and with ship-track gravity anomalies computed from the BGI gravity database.

KMS01 and the newest release of the KMS global marine free air gravity field, computed from ERS1 and GEOSAT satellite altimetry. Data for the Geodetic Missions of ERS and

GEOSAT have been used as well as for ERM60-63 of ERS2. The ERS ERM data (repeat 1-85) from the NASA Pathfinder project have also been used to ensure complete coverage in arctic and antarctic regions. (Andersen et al., 2003). KMS grids are 2 arc-minute by 2-arc minute gravity grids and they have been computed via conversion of marine geoid heights using the inverse Stokes's formula. Sub-grids were extracted from the grids over the study area. The statistics of the gravity anomalies for each grid, after land gravity anomalies were removed using the grdlandmask option in The Generic Mapping Tools (GMT) (Wessel and Smith, 1998) can be seen in Table 4.

Table 4. Statistics of KMS01 and KMS02, grids, their differences and ship-tracks gravity anomalies offshore Argentina Unit: [mGal]

	min	*max*	*mean*	σ
KMS01	-137.57	130.77	4.41	±25.59
KMS02	-134.26	131.47	4.39	±25.90
Shipborne data	-133.03	142.57	4.01	±28.64
KMS02-KMS01	-41.37	64.17	-0.02	±4.15

From Table 4 we can see, that both KMS models have similar statistics and the shipborne gravity anomalies data have a comparable range. The statistics of the differences between KMS02 and KMS01 can also be seen in Table 4 and it is depicted in Figure 2. From Figure 2, the larger differences occur over the South American-Scotia plate boundary and the edge of the continental shelf off Argentina. The KMS gravity anomalies were bilinear interpolated to the locations of the shipborne data. Table 5 presents the statistics of the differences between both grids and the 12823 shipborne gravity points using program geoip from the GRAVSOFT software (Tscherning et al., 1992). Plotting the differences between the two different KMS grids and the shipborne marine gravity anomalies, we conclude that the large differences correspond to the same ship-tracks. Due to the uncertain quality of the ship-track data, they should be used with caution to provide any reliable indication of the quality of the altimeter grids.

Table 5. Statistics of the differences between KMS grids and the shipborne marine gravity anomalies. Unit: [mGal]

	min	*max*	*mean*	σ
KMS01-shipborne	-61.47	67.74	0.99	±10.31
KMS02-shipborne	-63.67	66.31	1.25	±9.99

2.3 Combined solution using MIMOST

The estimation of the combined geoid solution was carried out using the MIMOST method in a smaller area between 40ºS to 50°S in latitude and 294°E to 304°E in longitude. The inputs of MIMOST were two residual gravimetric geoid heights (one with shipborne gravity data fill in with KMS01 and the other fill in with KMS02) and the residual altimetric geoid heights prior to the contribution of the geopotential model was restored in order to avoid long wavelength errors. Since, there is no information available about the input errors of both the altimetric and gravimetric models and these errors are necessary to apply the MIMOST method, simulated noises are used as input errors (Vergos et al., 2005b). The input errors for each dataset (white noise) were generated using the standard deviation of 19 cm for the altimetric geoid heights and 21 cm standard deviation for the gravimetric solutions. The final solution from the combined method as well the output error Power Spectral Density (PSD) function was estimated according the following equations:

$$\hat{X}_0 = \hat{H}_{x_0 y_0} Y_0 = H_{xy}[P_{y_o y_o} - P_{mm}]P_{y_0 y_0}^{-1} Y_0 \tag{2}$$

$$P_{\hat{e}\hat{e}} = [H_{xy}(P_{y_0 y_0} - P_{mm}) - \hat{H}_{x_0 y_0} P_{y_0 y_0}](H_{xy}^{*T} - \hat{H}_{x_0 y_0}^{*T}) + \hat{H}_{x_0 y_0} P_{mm} H_{xy}^{*T} \tag{3}$$

where $\hat{X}_o$ is the spectrum of the combined solution, Y_o is the input observation spectrum, m is the input error spectrum, H_{xy} is the theoretical frequency operator that connects the pure input y (the pure inputs are Ngrav with KMS01; Ngrav with KMS02 and Nalt) and the output signal X can be Ncomb (KMS01) or Ncomb (KMS02), $\hat{H}_{x_o y_o}$ is the optimum frequency impulse response function, $P_{y_o y_o}$ is the input observation PSD and P_{mm} is the input noise PSD.

Table 6 shows the statistics of the altimetric geoid, the gravimetric geoid with KMS01 and with KMS02 and the MIMOST combined solutions in the inner area.

Table 6. Statistics of the geoid models in the inner area. Unit:[m].

	min	*max*	*mean*	σ
Nalt	0.794	14.663	10.246	±3.279
Ngrav with KMS01	1.079	14.715	10.201	±3.088
Ngrav with KMS02	1.076	14.722	10.202	±3.087
Ncomb (KMS01)	0.788	14.618	10.247	±3.278
Ncomb (KMS02)	0.785	14.618	10.247	±3.278

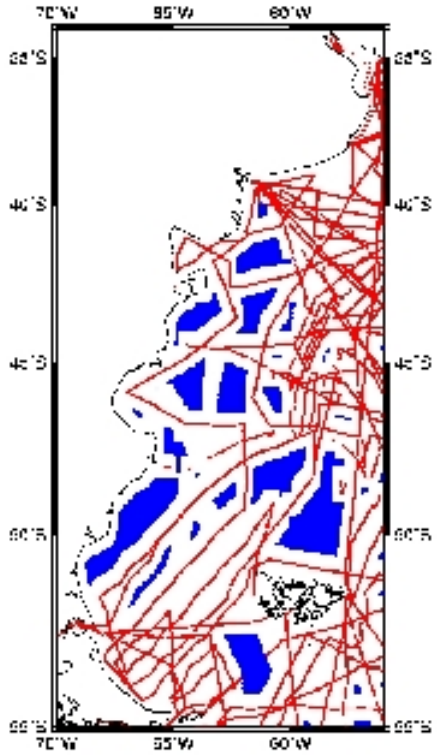

Figure 1: Gravity data distribution

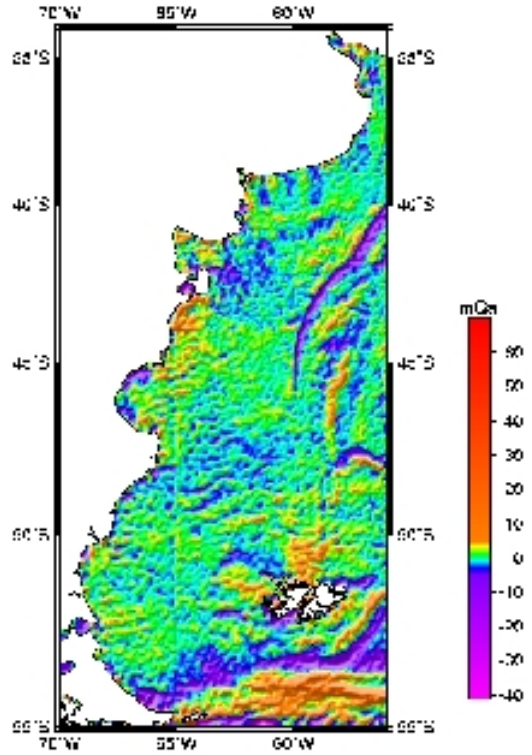

Figure 2: KMS02-KMS01 in Argentina

3 Validation of the estimated geoid models

For the validation of the estimated geoid solutions, stacked T/P SSHs were used together with the previous geoid models computed with EGM96 (Tocho et al., 2005). T/P provides repeated observations over the same tracks approximately every 10 days. For the comparisons stacked data was used because stacked T/P SSHs are known for their high accuracy and they

are close to the geoid dataset because the sea surface variability present in the SSHs have been reduced during the stack process. The differences between stacked SSHs from the 3rd year of the T/P mission and the estimated geoids were computed and minimized all possible datum inconsistencies and systematic distortions on the data using a four-parameter similarity transformation model, as (Heiskanen and Moritz, 1967):

$$N^{T/P} = N^{i} - b_0 \cos\varphi\cos\lambda - b_1 \cos\varphi \sin\lambda - b_2 \sin\varphi - b_3 \quad (4)$$

where $N^{T/P}$ is the stacked T/P SSHs, N^{i} is a gravimetric, altimetric or combined geoid height depending on the solution under consideration and the parameters b_o, b_1, b_2 and b_3 were calculated using a least squares technique.

Also comparisons were performed using a 3rd order polynomial model referred to the multiple regression equation (MRE) given in Fotopoulos (2003):

$$N^{T/P} = N^{i} - \sum_{m=0}^{M}\sum_{n=0}^{N} (\varphi - \varphi_0)^{n} (\lambda - \lambda_0)^{m} x_q \quad (5)$$

where $\varphi_0.\lambda_0$ are the mean values of the latitude and longitude of the T7P SSHs and xq contains the q unknown coefficients, q varies according to the number of terms up to a maximum of q = (N+1)(M+1).

These models are used in the same sense as in the land case where we want to adjust GPS/Leveling geoid heights with gravimetric geoid solutions. We assume that a four-parameter model or a third order polynomial model can describe the actual differences between T/P and our geoids; we treat the differences as they are due to the use of different datum in T/P and our geoid models and such parametric models manage to reduce the differences. From the results tabulated in Table 7, we conclude that the use of a 3rd order polynomial model is preferable compared to that of the use of the four-parameter transformation.

Table 7. Geoid height differences between the estimated models and T/P SSHs in the inner area. Unit: [m]. (before and after bias and tilt fit)

	min	*max*	*mean*	σ
Nalt-T/P SSHs	-1.15	1.15	0.15	±0.20
After a3rd order polynomial model	-1.06	1.20	0.00	±0.19
After a four-parameter similarity transformation model	-1.21	1.09	0.00	±0.20
Ngrav (KMS01)-T/P SSHs	-0.66	1.05	0.20	±0.28
After a 3rd order polynomial model	-0.80	0.85	0.00	±0.21
After a four-parameter similarity transformation model	-1.18	0.57	0.00	±0.23
Ngrav (KMS02)-T/P SSHs	-0.67	1.05	0.20	±0.28
After a3rd order polynomial model	-0.80	0.84	0.00	±0.21
After a four-parameter similarity transformation model	-1.19	0.57	0.00	±0.23
Ncomb (KMS01)-T/P SSHs	-1.16	1.11	0.15	±0.20
After a 3rd order polynomial model	-1.04	1.18	0.00	±0.19
After a four-parameter similarity transformation model	-1.20	1.05	0.00	±0.20
Ncomb (KMS02)-T/P SSHs	-1.16	1.11	0.15	±0.20
After a 3rd order polynomial model	-1.04	1.18	0.00	±0.19
After a four-parameter similarity transformation model 4P	-1.20	1.05	0.00	±0.20

Based on these results we conclude that there are no differences in the gravimetric geoid solutions computed using either KMS01 or KMS02 gravity anomalies and this fact is also reflected in the result of the combined solutions using the MIMOST method. The altimetric geoid and the combined solutions present the same differences with respect to the T/P SSHs.

The combined solution also improves the pure gravimetric solution to about ± 2 cm in terms of the standard deviations of the differences with stacked T/P SSHs.

Figure 3 depicts the MIMOST combined solution for the area under study calculated using the residual gravimetric geoid filled in with KMS01 data, as it is the same data used to derive the oldest solution computed with EGM96. From Table 8, we also conclude from comparisons made with the older solutions computed with EGM96 geopotential model (Tocho et al., 2005) and T/P SSHs for the same area, that the use of the new "combined" EGMs improves the results in ±1 cm in terms of the σ for the pure altimetric solutions, ±2 cm in terms of the σ for the pure gravimetric solutions and ±3 cm in terms of the σ for the combined solutions.

Table 8. Geoid height differences between the estimated models and T/P SSHs in the inner area, calculated with EGM96. Unit: [m]. (after bias and tilt fit, using a 3rd order polynomial model

EGM96	*min*	*max*	*mean*	σ
Nalt-T/P SSHs	-1.07	1.11	0.00	±0.20
Ngrav-T/P SSHs	-1.00	1.35	0.00	±0.23
Ncomb-T/P SSHs	-0.80	1.39	0.00	±0.22

It is worth mentioning, that the σ of the differences for the comparisons with the altimetric models is quite high, at the ±20 cm level, while a value close to ±9 cm would be expected based on previous studies (Li and Sideris, 1997; Vergos, 2002). Plotting the differences, it was noticed that their largest and smallest values are located close to the coastline and in an area where the effect of the SSV is very high. The standard deviations of the differences were reduced to about ±5 cm to ±9 cm when some T/P SSHs points were not considered. The same improvement was achieved for the gravimetric and combined models. It can be concluded that by only stacking the T/P data the effect of the SSV cannot be completely removed so the SSHs are not representative to make comparisons. Perhaps, the T/P data has to be low-pass filtered in their along –track direction to remove the remaining oceanic effect.

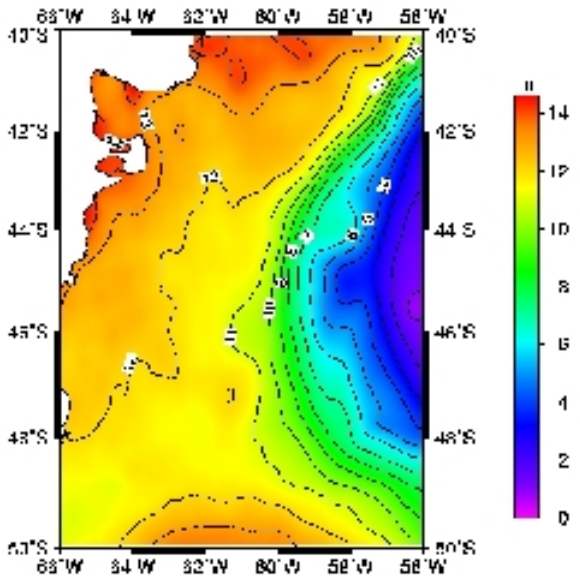

Figure 3: The MIMOST solution

4 Conclusions

Having determined a pure altimetric geoid model and gravimetric geoid height solutions for the Atlantic coastal region of Argentina, a combined solution using MIMOST method has been computed for a reduced area. The MIMOST method used for the optimal combination of heterogeneous data improves by ±2 cm the gravimetric only geoid model. The comparison with the old solution computed with EGM96 improves the results by ±1 cm for the altimetric geoid, ±2 cm for the gravimetric solutions and ±3 cm for the combined ones. This is an indication that the new EGM is slightly better than EGM96 geopotential model to use as reference field.

For the determination of the optimal marine geoid model in the area under study, a detailed analysis of the combination of land and marine gravity data on the coastline has to be carried out.

References

Andersen O.B. and Knudsen P. (1998): Global gravity field from ERS1 and Geosat geodetic mission altimetry, Journal Geophysical Research, vol. 103, no. C4, pp. 8129-8137.

Andersen OB, Knudsen P, Trimmer R. (2003): Improved high-resolution altimetric gravity field mapping (KMS02 Global marine gravity field), International Association of Geodesy Symposia, vol. 128, Sanso F. (Ed.), Springer. Proceedings of the Symposium 128: A window on the future of Geodesy, Sapporo, Japan, June 30-July 11, 2003, pp. 326-331.

Andritsanos V.D., Tziavos I.N. (2002): Estimation of gravity field parameters by a multiple input/output system, Physics and Chemistry of the Earth, Part A, vol. 25, no. 1, pp. 39-46.

AVISO User Handbook (1998): Corrected Sea Surface Heights (CORSSHs). AVI-NT-011-311-CN, Edition 3.1.

BGI (2001) : Personal communication.

Dahl O.C., Forsberg R. (1998): Geoid models around Sognefjord using depth data. Journal of Geodesy, vol. 72, pp. 547-556.

Forsberg R. (1984): A study of terrain corrections, density anomalies and geophysical inversion methods in gravity field modeling, Report of the Department of Geodetic Science and Surveying no. 355, The Ohio State University, Columbus, Ohio

Fotopoulos G. (2003): An analysis on the optimal combination of geoid, orthometric and ellipsoidal height data, PhD. Thesis, University of Calgary, Department of Geomatics Engineering, UCGE Reports Number 20185.

Heiskanen W.A., Moritz H. (1967): Physical Geodesy. WH Freeman, San Francisco.

Lemoine, F.G., Kenyon, S.C., Factim, J.K., Trimmer, R.G., Pavlis, N.K., Chinn, D.S., Cox, C.M., Klosko, S.M., Luthcke, S.B., Torrence, M.H., Wang, Y.M., Williamson, R.G., Pavlis, E.C., Rapp, RH. and Olson, T.R. (1998): The development of the joint NASA GSFC and

the National Imagery and Mapping Agency (NIMA) Geopotential Model EGM 96. Pub. Goddard Space Flight Center.

Li Y.L. and Sideris M.G. (1997): Marine gravity and geoid determination by optimal combination of satellite altimetry and shipborne gravimetry data, Journal of Geodesy, vol. 71, pp. 209-216.

Li Y.C. (1993): HFTGVBP Software package for the solution of GVBP by means of fast Hartley/Fourier Transform TOPOGEOP Software packages to evaluate the TOPOgraphic effects on GEOdetic /GEOPhysical Observation Department of Geomatics Engineering The University of Calgary.

Sideris M.G. (1996): On the use of heterogeneous noisy data in spectral gravity field modeling methods, Journal of Geodesy, vol. 70, pp. 470-479.

Smith W.H.F and Sandwell D.T. (1997): Global Sea Floor Topography from Satellite Altimetry and Ship Depth Soundings, Science Magazine, vol. 277, Issue 5334.

Strang van Hees G. (1990): Stokes' formula using fast Fourier techniques. Manuscripta Geodaetica, vol. 15, pp. 235-239.

Tocho C., Vergos G.S., Sideris M.G. (2005): Optimal marine geoid determination in the Atlantic coastal region of Argentina. In: Sansó F (ed) International Association of Geodesy Symposia, Vol. 128, "A Window on the Future of Geodesy", Springer - Verlag Berlin Heidelberg, pp. 380-385.

Tscherning C.C., Forsberg R., Knudsen P. (1992): The GRAVSOFT package for geoid determination. In: Holota P., Vermeer M. (Eds), 1st Continental Workshop on the Geoid in Europe, Prague, June 7-9, 1993, pp. 327-334.

Vergos G.S. (2002): Sea Surface Topography, Bathymetry and Marine Gravity Field Modeling, MSc Theses Dissertation, Dept of Geomatics Engineering, University of Calgary, UCGE Reports 20157, Calgary, Alberta.

Vergos G.S., Tziavos I.N., Sideris M.G. (2004): On the validation of CHAMP- and GRACE-type EGMs and the construction of a combined model, Presented at the Joint CHAMP/GRACE Science Meeting, July 6-8, Potsdam, Germany.

Vergos G.S., Tziavos I.N., Andritsanos V.D. (2005a): On the Determination of Marine Geoid Models by Least Squares Collocation and Spectral Methods Using Heterogeneous Data. In: Sansó F (ed) International Association of Geodesy Symposia, Vol. 128, "A Window on the Future of Geodesy", Springer - Verlag Berlin Heidelberg, pp 332-337.

Vergos G.S., Tziavos I.N., Andritsanos V.D. (2005b): Gravity Data Base Generation and Geoid Model Estimation Using Heterogeneous Data. In: Jekeli C, Bastos L, Fernandes J (eds.) International Association of Geodesy Symposia, Vol. 129, "Gravity Geoid and Space Missions 2004", Springer – Verlag Berlin Heidelberg, pp. 155-160.

Wessel P. and Smith W.H.F. (1998): New improved version of The Generic Mapping Tools released. EOS Trans 79(47): 579.